JOURNAL OF SYNCHROTRON RADIATION
ISSN 1600-5775

One way only to synchrotron light sources upgrade?

Simone Di Mitri*

Elettra – Sincrotrone Trieste SCpA, Basovizza, Trieste I-34149, Italy. *Correspondence e-mail: simone.dimitri@elettra.eu

Received 10 April 2018
Accepted 1 June 2018

Edited by M. Eriksson, Lund University, Sweden

Keywords: synchrotron radiation; free-electron laser; short pulse; diffraction limit; storage ring; electron-optics design.

The last decade has seen a renaissance of machine-physics studies and technological advancements that aim to upgrade at least 15 synchrotron light sources worldwide to diffraction-limited storage rings. This is expected to improve the average spectral brightness and transversally coherent fraction of photons by several orders of magnitude in the soft- and hard-X-ray wavelength range, at the expense of pulse durations longer than ∼80 ps FWHM. This paper discusses the compatibility of schemes for the generation of sub-picosecond photon-pulse durations in synchrotron light sources with standard multi-bunch user operation and, in particular, diffraction-limited electron optics design. The question of this compatibility is answered taking into consideration the storage ring beam energy and the constraint of existing synchrotrons' infrastructure. An alternative scheme for the upgrade of medium-energy synchrotron light sources to diffraction-limited storage rings and the simultaneous production of picosecond-long photon pulses in a high-gain free-electron laser scheme are illustrated.

1. Introduction

After almost 15 years from its first presentation in 1995 (Einfeld *et al.*, 1995), the concept of diffraction-limited storage rings (DLSRs) has started driving worldwide upgrade projects of so-called third-generation synchrotron light sources in the electron-beam energy range 2.5–6 GeV (Borland, 2014). The last decade has therefore seen a renaissance of machine-physics studies and technological advancements that aim to put these new light sources in operation in the time frame 2020–2030 (Hettel, 2014). An improvement of the average spectral brightness and transversally coherent fraction of photons by several orders of magnitude in the soft and hard X-ray wavelength range is promised. Third-generation synchrotron light sources, built with optimized low-emittance lattices and making extensive use of undulators, have a wide domain of application because of the unique properties of synchrotron radiation; such properties include spectral coverage from THz to hard X-rays, high average photon flux, high stability and polarization control. On top of this, DLSRs promise a substantial step forward in all the experimental techniques based on higher coherence and coherent photon flux, high average brilliance (*e.g.* coherent diffraction), small spot size (*e.g.* micro- and nano-focus beamlines) and small divergence (*e.g.* scattering). Such a breakthrough, however, comes at the cost of bunch durations typically longer than ∼80 ps FWHM, as explained below.

The last decade has also seen the advent of linac-driven high-gain free-electron lasers (FELs) (Fritz & Yabashi, 2017). They are pushing the peak spectral brilliance and peak power of EUV and hard X-ray photon pulses to unprecedented levels, typically up to nine orders of magnitude higher than in

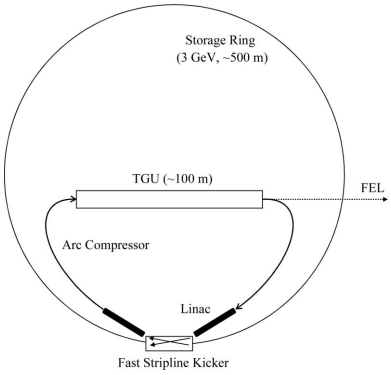

synchrotron light sources. These performances are associated with full transverse and longitudinal coherence (the latter presently achieved only down to wavelengths of a few nanometres) (Prince *et al.*, 2016), and pulse durations in the range ∼0.1–500 fs (Reis, 2016), whereas the pulse repetition rate, now targeting 1 MHz, is typically some orders of magnitude lower than in synchrotron light sources.

Synchrotron-radiation X-rays can be used to resolve the structure of matter on the molecular- or atomic-length scale (∼0.1–1 nm). To study the dynamical properties of matter in this spatial domain, an X-ray probe with a duration that is shorter than the process that is being studied is required. While single-shot images of samples can be recorded if the light pulse is sufficiently short and intense, such as in FELs, less intense pulses at high repetition rate can be used to track fast-moving objects such as aerosols in free-flight or the evolution of non-equilibrium states, while minimizing the sample damage. In fact, pulse duration at the picosecond time scale is needed for probing charge transfer dynamics, orbital, spin and lattice degrees of freedom in materials on the nanometre length scale. The investigation of reversible dynamics in molecular systems of different materials requires a non-destructive photon–matter interaction that is often not possible at FELs, whose multi-GW peak power, in some cases up to the TW level, can profoundly damage the sample. Even in cases of the sample surviving a relatively high photon flux, space charge effects in photo-electron spectroscopy up to ablation may seriously compromise the collection of information on the sample properties. Finally, the relative wavelength tunability in FELs is typically limited to a few percent, whereas, for example, extended X-ray absorption fine structure (EXAFS) and similar experimental techniques require access to a much wider spectral range. Storage rings look like the most suitable light source for such studies, where the reduced peak photon flux is accompanied by the 10–500 MHz repetition rate, and wide-wavelength tunability is provided, *e.g.* by dipole magnets and variable-gap insertion devices (IDs) in a series.

The historical development of synchrotron light sources (Williams & Herman, 2015) shows a trend in the equilibrium electron bunch length towards shorter and shorter values, with a reduction of one order of magnitude in 40 years [see, for example, Fig. 1.6 of Martin (2011)]. While this picture confirms the interest of the synchrotron radiation community in shortening the X-ray pulse duration, the advent and continuous development of high-gain FELs raises the question of whether the production of pulses in the (sub-)picosecond time domain should become an exclusive operating mode of these coherent and powerful light sources.

The duration of a radiation pulse spontaneously emitted by an ultra-relativistic electron bunch either in a dipole magnet or an ID (referring here to both wigglers and undulators) reflects that of the source. This is typically not shorter than 10 ps (r.m.s. value) in third-generation synchrotron light sources and at least about three times longer in DLSRs. The natural bunch length is primarily set by the radiofrequency (RF) of the accelerating cavities, usually operating at 100 or 500 MHz. Additional bunch lengthening is commonly induced by the electric field of a higher harmonic cavity with the aim of suppressing either transverse or longitudinal beam instabilities, and increasing the beam Touschek lifetime. In addition to this, bunch lengthening is mandatory in DLSRs for minimizing the transverse emittance growth otherwise induced by intra-beam scattering in high-charge-density bunches (Leemann, 2014). It is therefore a general trend of low-emittance rings for increasing either the spectral brilliance or the fraction of coherent photons in the X-ray wavelength range at the expense of time resolution.

In the following, a compromise between stored electron beams at the diffraction limit in the soft X-ray wavelength range and short-bunch duration is investigated. In §2 the relevance of the beam horizontal emittance to the photon brightness (or brilliance) is recalled. While in the existing literature a scaling of energy-normalized horizontal emittance is given *versus* the ring circumference (Liu & Westfahl, 2017), we present here a scaling law which explicitly relates geometric emittance and beam energy, where the dependence of the circumference on the energy is in turn the result of a fitting applied to existing data. This allows us to quantify the 'emittance gap' that third-generation synchrotron light sources should fill in order to approach the diffraction limit, exclusively as a function of the stored beam energy. In §3 we review, in short, techniques for the stable production of sub-picosecond-long photon pulses in storage rings and, by relying on the findings of the previous sections, discuss the compatibility of such schemes with diffraction limit electron-optics designs. Finally, a high-gain FEL driven by the stored beam is revisited in §4, and performance in the EUV and soft X-ray are anticipated. In §5 we summarize the expected and typical performance of short-pulse schemes and their compatibility with low-emittance optics. Conclusions are given in §6.

2. Diffraction limit and emittance scaling

2.1. Definitions

The photon brightness or brilliance (Kim *et al.*, 2017) is the main quality factor for a synchrotron light source and is defined as the photon flux per unit area per unit solid angle at the source,

$$B = \frac{\Phi}{4\pi^2 \Sigma_x \Sigma_{x'} \Sigma_y \Sigma_{y'}}, \tag{1}$$

where Φ is the total photon flux per 0.1% bandwidth and Σ_s are the quadratic convolution of the electron r.m.s. beam size (Σ_x, Σ_y) and divergence ($\Sigma_{x'}$, $\Sigma_{y'}$) and the natural photon r.m.s. size and divergence, respectively The electron r.m.s. beam size and divergence depend on the lattice. If a dispersion-free region is considered, *e.g.* an undulator where the average dispersion is null, it is found that the brilliance is maximized when the electron-beam betatron functions are matched to those equivalently defined for the photon beam (assuming Gaussian spatial and angular distributions of the

two beams). For a planar undulator of length L, this means $\beta_x = \beta_y = \beta_{\rm ph} = L/\pi$ (Bazarov, 2012), and the peak brightness

$$\hat{B} = \frac{\Phi}{4\pi^2\left[\varepsilon_x + (\lambda/4\pi)\right]\left[\varepsilon_y + (\lambda/4\pi)\right]}, \qquad (2)$$

where $\lambda/4\pi$ is the photon-beam emittance. It is therefore clear that reducing the electron beam emittance will increase the brilliance of the photon beam. This is true until we reach the so-called diffraction-limited emittance, $\varepsilon_{x,y} \leq \varepsilon_{{\rm ph};\,x,y} = \lambda/4\pi$, which implies an electron-beam emittance of less than 10 pm rad in both planes for diffraction-limited operation at λ = 1 Å. Reducing the emittance even further will not significantly increase the brilliance, at least at those wavelengths where the denominator in equation (2) will be dominated by the photon-beam size and divergence. The transverse coherence follows a similar dependence with the emittance. The coherent photon flux is a measure of the transverse coherence of the radiation pulse and turns out to be $\Phi_{\rm coh} = B(\lambda/2)^2$. Accordingly, the coherent fraction of emitted photons $F = \Phi_{\rm coh}/\Phi$ is unitary for zero electron-beam emittance.

We note that brilliance is not the only figure-of-merit for these light sources and actually a large fraction of users are instead interested in increasing the flux, without necessarily increasing the brilliance. These users' requirements can be equally served by increasing the operating currents in existing third-generation lattices rather than decreasing the emittance. For any given synchrotron infrastructure and assuming a multi-bunch filling pattern already >95%, a higher average beam current can only be gained by increasing the bunch charge. Intra-beam scattering processes would imply, in this case, a higher RF voltage for a larger momentum acceptance, more efficient single-bunch and multi-bunch feedback systems, and reduced machine impedance (this is, however, determined by the geometry and materials of the vacuum vessel). A practical limit to the maximum average stored current, which is to date at the level of ∼500 mA for a 3 GeV beam, is set by the thermal stability of the storage ring components, and the damage threshold of mirrors used for X-ray photon transport to the beamlines.

2.2. Scaling laws

Most of the multi-GeV synchrotron light sources already have vertical emittances at the diffraction limit for radiation wavelengths around 0.1 nm or longer, whereas the horizontal emittance is two or three orders of magnitude higher (Liu & Westfahl, 2017). Pushing the horizontal emittance to the diffraction limit implies major efforts in magnetic, mechanical and vacuum technology, beam-based control systems and accelerator design. The latter has typically to trade-off a strong-focusing lattice to reach an ultra-low emittance, a sufficiently large dynamic aperture for either high-beam-injection efficiency or beam lifetime, and a relatively compact accelerator footprint (Hettel, 2014).

It is well known that, for a ring with a periodic lattice based on isomagnetic achromatic cells, the minimum natural emittance is given by $\varepsilon_x = C_{\rm q} F E^2 \theta^3/m_{\rm e}^2 \simeq E^2/N_{\rm d}^3$, where $C_{\rm q}$ = 3.84 × 10^{-13} m, $\theta = 2\pi/N_{\rm d}$ is the dipole bending angle, $N_{\rm d}$ is the total number of dipoles in the ring and F = 0.02–0.07 depending on the linear-optics cell design (related to quadrupoles focusing). Additional considerations related to non-linear optics and beam stability, as well as to the need of practical cell sizes, commonly increase the theoretical value of F up to ∼0.2. By virtue of the energy dependence of the electron-beam emittance, $\varepsilon \propto E^2$, and of the synchrotron-radiation wavelength, $\lambda \propto E^{-2}$, it is commonly perceived that lower-energy synchrotron light sources are favored in approaching the diffraction limit at critical wavelengths, with respect to higher-energy rings. At the same time, higher-energy rings typically exploit larger ring circumferences and therefore can host a relatively large number of dipole magnets, which tends to lower the emittance. Also, more room might be available with respect to lower-energy compact rings for more and stronger-focusing magnets devoted to building up a low-emittance lattice. In short, the ring circumference is recognized in playing a role in the emittance evaluation.

A quantitative estimation of the 'gap' to be covered by third-generation light sources to fully reach the diffraction limit is given below, and such a gap is shown as an exclusive function of the electron-beam energy. We start noticing that the ring circumference of the majority of existing facilities, many of them based on double- or triple-bend achromatic cells, is approximated by the relationship $C \simeq 7 l_{\rm d} N_{\rm d}$, where $l_{\rm d}$ is the dipole length and the spread of the numerical coefficient is about 20% over a representative ensemble. At the same time, a linear fit of the circumference to the beam energy suggests $C\,[{\rm m}] \simeq 125\,E\,[{\rm GeV}]$ (Liu & Westfahl, 2017). By placing those expressions into $\theta = 2\pi/N_{\rm d}$, and then inserting into the theoretical expression for the minimum horizontal emittance, we obtain

$$\varepsilon \simeq \frac{C_{\rm q}\tilde{F}}{m_{\rm e}^2}\left(\frac{14\pi l_{\rm d}}{125}\right)^3 \frac{1}{E}. \qquad (3)$$

Fig. 1 shows that, by choosing the realistic value $\tilde{F} = 0.19$ and $l_{\rm d}$ = 1 m as fitting parameters in equation (3), the horizontal emittance of third-generation light sources can be predicted within a factor of two. The limited accuracy of prediction of equation (3) is still of some help for the discussion, when compared with an emittance reduction by at least one order of magnitude to match the diffraction limit.

The emittance given by equation (3) is now compared with the photon-beam emittance, at the wavelength of interest. In a short planar-polarized undulator, the on-axis fundamental emission is centered at $\lambda\,[{\rm nm}] = \left\{1.306\lambda_u\,[{\rm cm}]\,(1 + K^2/2)\right\}/(E^2\,[{\rm GeV}])$, where $\lambda_{\rm u}$ is the undulator period and $K = 0.934\,\lambda_{\rm u}\,[{\rm cm}]\,B\,[{\rm T}]$ is the undulator parameter associated with the undulator peak magnetic-field. In Table 1 we consider three realistic sets of ID parameters in the linear polarization configuration. It is worth recalling that users often rely on undulator emission at harmonic orders as high as ∼5–30 when the electron-beam energy and the

Table 1
Three sets of parameters of a linearly polarized undulator: undulator period, undulator parameter and on-axis fundamental undulator wavelength.

λ_u (cm)	K	λ_f (nm) at 3 GeV
10	10	74
5	5	9.8
2.5	2	1.1

undulator period are not suitable for direct X-ray emission at the fundamental wavelength.

The ratio of the horizontal natural-equilibrium emittance [equation (3)] over the diffraction-limited emittance *versus* electron-beam energy is illustrated in Fig. 2 (top plot), for the three IDs in Table 1. The ratio is linearly proportional to the beam energy (the figure is on a semi-log scale). Facilities in the energy range $E > 3$ GeV typically target high flux at hard X-ray wavelengths; they are therefore well represented by the green curve. This plot says on an approximate but still quantitative basis that, in order to reach the diffraction limit, an emittance reduction by at least a factor of ∼30–100 has to be accomplished. The red curve in the same plot shows that existing rings at $E < 3$ GeV can approach the diffraction limit for a good portion of the EUV and soft X-ray user community with a reduction in the horizontal emittance by a factor of ∼10. By considering a higher harmonic jump of up to ten for the listed wavelengths, an emittance-reduction factor up to ∼1000 and ∼100 is expected for the high- and low-energy-range machines, respectively.

Fig. 2 (bottom plot) shows, as a practical example, the equilibrium horizontal emittance of a 500 m-circumference synchrotron light source based on a double-bend achromatic cell (DBA) lattice, re-scaled with number of dipoles per cell at fixed circumference length, for diverse beam energies (red lines). The crossing point of the emittance lines with the curves of the undulator resonant wavelengths (blue lines, ID parameters in Table 1) identify the beam energy at which the diffraction limit is achieved. This plot suggests that light sources at energies higher than 3–4 GeV would be asked to incorporate a multi-bend lattice with at least seven, eight or more dipole magnets per cell (see the crossing point of the blue and red dotted line). Light sources at $E < 3$ GeV would most likely reach the diffraction limit in the soft-X-ray range with six or so dipoles per cell.

It is then conceivable that an upgrade of storage rings at beam energies lower than 3 GeV, targeting a more relaxed emittance reduction, may be compatible with electron-optics design and installation of new hardware for the generation of short (picosecond and sub-picosecond) photon pulses.

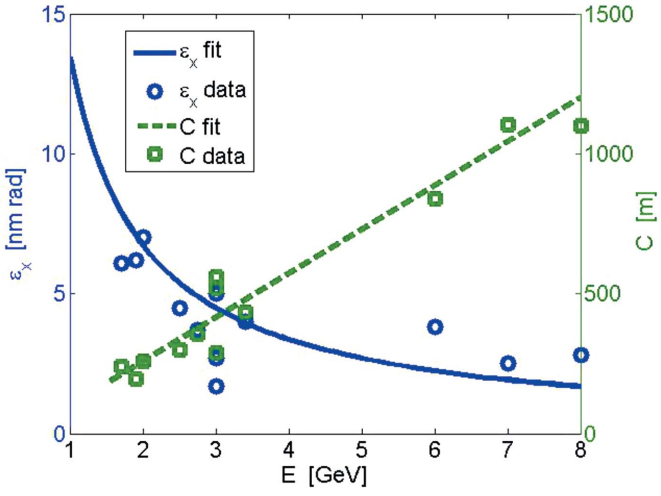

Figure 1
Horizontal natural emittance (ε_x, blue) and storage-ring circumference (C, green) *versus* electron-beam energy of a representative ensemble of existing third-generation synchrotron light sources (Feikes *et al.*, 2004) (BESSY II, ALS, Elettra, ALBA, Soleil, Diamond, SLS, TPS II, SSRF, APS, ESRF, SPring-8). Lines are fits to the experimental values as discussed in §2.2.

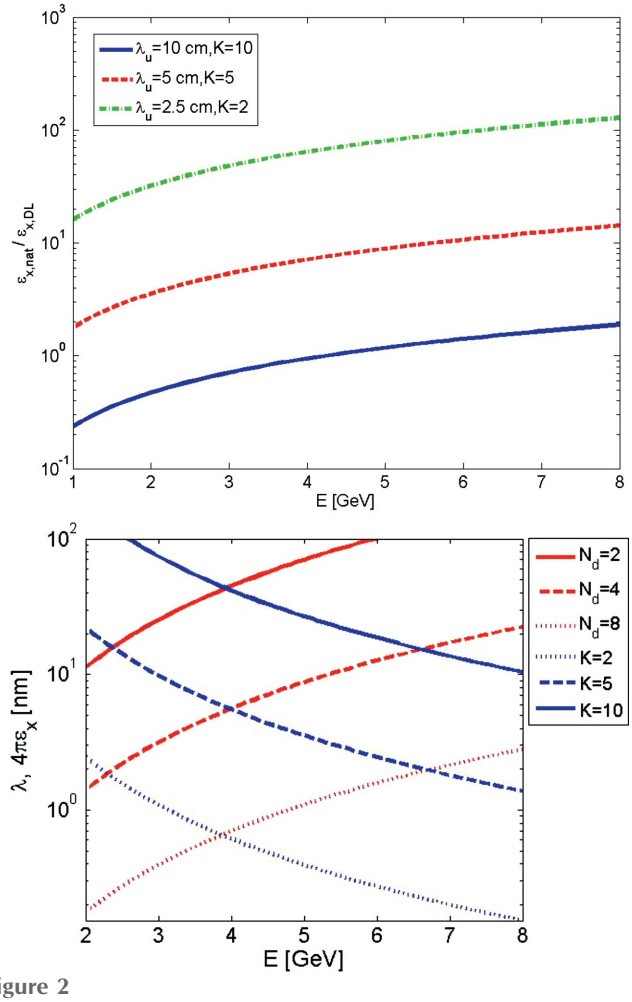

Figure 2
Top: ratio of the equilibrium horizontal emittance of existing third-generation synchrotron light sources over the diffraction-limit value, at three undulator radiation wavelengths defined by the parameters in the legend (see also Table 1). The three wavelengths at the beam energy of 3 GeV are λ = 74 nm (blue), 10 nm (red) and 2 nm (green). Bottom: equilibrium horizontal emittance of a 500 m-circumference synchrotron light source based on a DBA lattice re-scaled with the number of dipoles per cell over the same circumference, and with energy (red lines). The undulator wavelengths defined above *versus* beam energy are superimposed (blue lines).

3. Short-pulse schemes

Different schemes for the production of sub-picosecond photon pulses in synchrotron light sources can be found in the literature. Not all of them have been tested yet, and only a few of them look to be compatible with the preservation of relatively high photon brilliance. We recall here only those promising a stable production of short pulses, *i.e.* short photon pulses are generated by electron particle distribution at equilibrium. We mainly refer to the thesis by Martin (2011) for a more detailed description of the schemes and of their typical performance such as: (i) shortening electron bunches to $\sim$1 ps duration *via* either optics or RF gradient manipulation; (ii) transverse-to-longitudinal electron-bunch coupling induced by an RF deflecting cavity, and downstream selection of $\sim$1 ps photon-pulse duration; (iii) external laser-based methods such as femto-slicing and coherent harmonic generation (CHG), for $\sim$0.1 ps photon-pulse duration; and (iv) low-gain FELs.

3.1. Low-alpha optics

Stable shortening of the electron-bunch duration is provided by the so-called low-alpha operation (Robin *et al.*, 1993; Feikes *et al.*, 2004). This consists of tuning of the magnetic lattice, at fixed beam energy, in order to reduce the linear momentum compaction (α_c) of the storage ring, where the equilibrium bunch length scales as $\sigma_z \propto (\alpha_c/V_{RF})^{1/2}$, where V_{RF} is the RF peak voltage. The latter cannot be increased typically by more than a fraction of the nominal value because of hardware restrictions. Instead, a reduction of α_c by more than one order of magnitude was demonstrated for user operation and a minimum bunch length at the $\sim$1 ps level was recorded (Feikes *et al.*, 2004). The lower limit for the bunch length, even in the ideal case of an isochronous ring, is due to collective effects established at non-zero beam current, such as potential-well distortion, higher-order dependence of the bunch length on the beam energy spread (higher-order momentum compaction) and an increased sensitivity of closed-orbit motion to errors. Since the low-alpha mode implies a reduced bunch charge for avoiding the onset of the microwave instability in short bunches, the single-pulse radiation intensity is commonly reduced by several orders of magnitude with respect to the standard operation. A value of $\alpha_c \simeq 10^{-5}$ together with an accurate control of the second-order momentum compaction allows the simultaneous storage of short ($\sim$1 ps) and long bunches ($\sim$10 ps). The emitted synchrotron radiation can be spatially and angularly separated in dispersive regions of the lattice. Several attempts to establish low-alpha optics in third-generation synchrotron light sources have demonstrated that it usually goes in conflict with optics devoted to ultra-low emittance because of opposite constraints on the dispersion function in the dipole magnets. When optics prescriptions for a low emittance are retained, a large natural chromaticity is excited, thus resulting in large sextupole strengths and reduced dynamic and momentum aperture (Martin *et al.*, 2011).

3.2. RF voltage beating

A simultaneous and stable accumulation of $\sim$10 ps- and $\sim$1 ps-long bunches (r.m.s. values), available to all beamlines, is promised by the so-called RF voltage beating scheme (Wüstefeld *et al.*, 2011), which sees the installation of (at least) two superconducting high-gradient ($\sim$20 MV m^{-1}) RF cavities with slightly different frequencies in the L-band, in addition to the standard cavity devoted to beam acceleration. In order to minimize coupled-bunch transverse and longitudinal instabilities, the cavities shall be equipped with high-order-mode suppressors. Voltage and phase of the harmonic cavities are tuned in a way that their field adds up at even fixed points of the buckets train, leading to enhanced RF focusing and therefore bunch shortening, and cancel at the odd fixed points. A further reduction of the bunch length to sub-picosecond duration would be given by the combination of such strong RF focusing with low-alpha optics. Preliminary estimations of potential-well distortion and beam instabilities threshold for BESSY-II suggest an average bunch current of 0.8 (0.04) mA for 1.7 (0.4) ps r.m.s. bunch duration (Jankowiak *et al.*, 2016). If the low-alpha optics is not pursued, the nominal emittance at the nm rad level could also be preserved for the short bunches, at the expense of a lower charge. Top-up injection is still possible, where the strong RF gradient reduces by one order of magnitude the phase acceptance of injected bunches, and the energy acceptance becomes limited by the dynamic aperture and the low-gap ID vacuum chamber (Jankowiak *et al.*, 2016).

It is worth mentioning that a simpler approach to bunch shortening, at the expense of longer bunch durations compared with those discussed so far, is given by either a passive or active cavity, typically tuned at the third or fifth harmonic of the baseline RF (Chin, 1990). The harmonic cavity is set to produce an effect opposite to the bunch lengthening discussed in §2. Realistic compression factors are in the range 2–5 for peak voltage of 1–10 MV in synchrotron light sources at $\sim$3 GeV beam energy (Bartolini *et al.*, 2006). Some additional shortening might be achieved with the simultaneous adoption of low-alpha optics. Of course, the shorter the bunch then the higher the charge density becomes and the stronger the effect of intra-beam scattering on the transverse emittance (unless a proportional reduction of the bunch charge is accepted). This kind of operation has to take into consideration some efforts in suppressing transverse- and longitudinal-beam instabilities, which are usually suppressed by bunch lengthening. Touschek lifetime is predicted to lower in proportion to the bunch-length compression factor.

3.3. RF vertical deflection

Vertical deflection of the electron bunch with RF 'crab' cavities (Zholents *et al.*, 1999) gives a transverse kick that is correlated along the bunch, such that the bunch head and tail oscillate in opposite directions. The light emitted in an undulator is separated in the vertical plane in position (angular or spatial slicing) and time (chirped radiation). A short pulse can be extracted by either installing vertical slits

in the beamline or by compressing the chirped photon pulse using asymmetrically cut crystals. A second cavity is used to remove the kick imparted to the electron beam by the first cavity, thus confining the deflection to a small section of the storage ring. An improved version of this scheme (Zholents, 2015) requires two RF deflecting cavities with slightly different frequencies for producing time-dependent orbit deflection to a few selected electron bunches, without affecting the majority of the stored bunches. In this way several beamlines can select between receiving either high-brilliance long X-ray photon pulses from a standard electron bunch or short X-ray pulses with reduced brilliance. The ultimate pulse duration to be produced with this scheme is mainly limited by mechanical misalignment deflecting cavities, RF phase and voltage jitter. The minimum pulse duration, for any given deflecting voltage, requires an integer multiple of π-betatron phase advance between the first deflecting cavity and the undulator (to maximize the bunch head–tail angular separation), and between the two deflecting cavities (to perfectly cancel the vertical kick). Although limited to a region of the ring, which may include several bending cells, these optics constraints are likely to be in conflict with an ultra-low-emittance lattice, both in terms of optics design and available space. They are also prone to amplification of sextupole-induced optical aberrations. At the same time, by virtue of the local-electron-beam manipulation, the optics tuning for vertical deflection looks less invasive than the global modification required by low-alpha operation.

3.4. Femto-slicing

Femto-slicing (Zholents & Zolotorev, 1996; Schoenlein *et al.*, 2000) refers to the interaction of a ~0.1 ps-long UV laser with the stored electron bunch in a short undulator (modulator). The energy modulation induced upon the electrons at the laser wavelength translates into density modulation through a dispersive region of the lattice, and into transverse separation of the affected electrons. As a result, the light emitted by the un-modulated electrons travels in a different direction to that emitted by the energy-modulated particles, and can be blocked by aperture restrictions. The repetition rate of the short pulse is determined by the external laser, *e.g.* up to 100 kHz for tens of μJ per pulse at ~800 nm (Höppner *et al.*, 2015) and by the amount of (damping) time required by previous modulations to wash out (typically not shorter than 10 ms). In fact, beam stability requires that electrons are mixed within the bunch before the next interaction of the same bunch with the laser. As long as femto-slicing does not imply any manipulation of the electron bunch at equilibrium, it is in principle compatible with ultra-low-emittance lattices. In reality, the main conflict might be caused by the space of several meters required for setting up the laser–electron interaction. The number of photons per pulse is commonly $\leq 10^{-4}$-fold smaller than for a standard radiation source, because of the small amount of electrons interacting efficiently with the external laser (Zholents & Zolotorev, 1996).

3.5. Coherent harmonic generation

External seeding by a ~0.1 ps-long UV-laser pulse can generate intense EUV emission through coherent harmonic generation (CHG) in a single-pass configuration (Yu, 1991), such as optical klystron (OK) (De Ninno *et al.*, 2008) and echo-enabled harmonic generation (Stupakov, 2009; Evain *et al.*, 2012). The energy modulation induced by the electron-beam laser interaction in the modulator is translated into density modulation (bunching) at the same wavelength. For a large bunching factor at the fundamental wavelength, coherent emission at higher harmonics can be obtained at reduced intensity passing by an undulator radiator. Since the radiator is typically only a few metres long, the emission is far from any power saturation. Production of electron bunching at third or higher harmonics of the seed laser wavelength implies $K > 10$ for $E > 2$ GeV, and a modulator period longer than ~5 cm. Thus, issues related to the longitudinal occupancy of the undulator section similar to those discussed for the femto-slicing arise. Practical considerations for the undulator length and its minimum gap suggest a realistic case at beam energies lower than 3 GeV, as shown in Fig. 3. In addition, since coherent emission is based on a single pass of the electron beam through the undulator section, a bunch peak current >100 A is commonly required in order to obtain ~10^7–10^9 photons per pulse at wavelengths typically longer than ~100 nm for the OK scheme and ~20 nm for the echo-enabled scheme. This in turn implies single or few bunches operation of the synchrotron light source, where either the

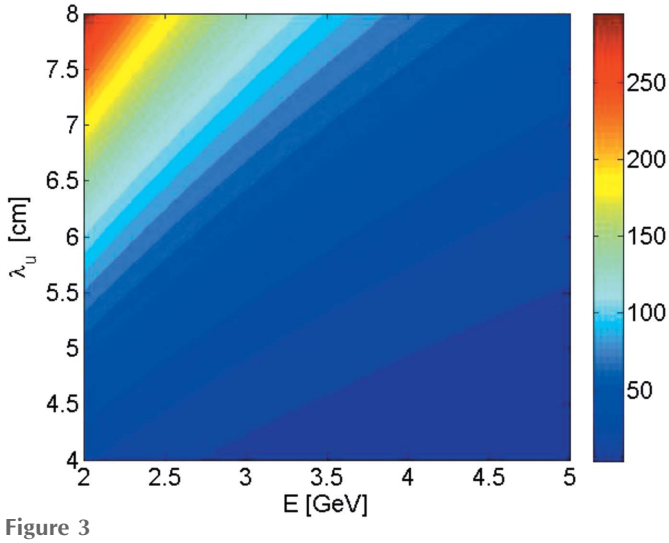

Figure 3
On-axis fundamental undulator wavelength in nanometers (color bar) *versus* undulator period and electron beam energy in the synchrotron light source. A hybrid undulator model with a full gap of 4 mm is assumed. For a gap of 7 mm the radiation wavelength is approximately doubled. The undulator parameter K is approximately linear with the undulator period and in the range 4–15. For CHG schemes, the modulator period has to match a seed laser wavelength presently available at wavelengths not shorter than ~240 nm. At beam energies below 3 GeV, this implies $\lambda_u > 8$ cm and 2–3 m in length. Similarly, beam energies lower than 3 GeV favor a more compact radiator. For example, emission at the third harmonic of the seed laser at 3 GeV requires $\lambda_u > 6.5$ cm and several meters in length.

natural-bunch duration in the absence of harmonic cavity or bunch shortening through harmonic cavity or low-alpha optics is adopted. The compatibility of these schemes with the standard user multi-bunch filling pattern is therefore compromised. The relatively high charge density may also induce some degradation of the transverse emittance by means of intra-beam scattering.

Recently, a more efficient optical manipulation of the electron beam for CHG down to ∼10 nm has been proposed (Feng & Zhao, 2017). The higher amount of bunching promised by this scheme would allow an increase of the number of photons per pulse by up to two orders of magnitude with respect to aforementioned solutions, for a given wavelength of emission. This might also imply some relaxed constraints on the bunch peak current at longer wavelengths (*e.g.* >50 nm) for a flux comparable with that of the schemes discussed above. Some concerns remain about the undulator length, beam energy, electron beam optics design, bunch length and emittance degradation analogous to those discussed above.

3.6. Low-gain FEL (optical cavity)

Almost fully coherent emission can be approached in a low-gain FEL, installed, for example, in a dedicated straight section or in a by-pass line internal to the synchrotron light source. In the optical cavity configuration (Dattoli *et al.*, 1998; Couprie, 1997), the weak electric field emitted in a short undulator at each passage of the electron bunch is cumulated over thousands of turns, until a quasi-stable and intense self-amplified FEL emission is established. The spectral threshold of the mirrors' reflectivity sets the lower limit of the FEL wavelength at ∼150 nm (Trovò *et al.*, 2002). In order for the electron beam to match the resonant emission at such wavelength, and assuming a minimum beam energy of 2 GeV, an undulator period of ∼10 cm and an undulator parameter $K \leq 10$ are needed. At the same wavelength, higher beam energies imply stronger K-values, typically associated with longer undulator periods and smaller undulator gaps. Because of either the maximum available space for accommodating the undulator (*e.g.* <4 m for a dispersion-free typical straight section) or the minimum tolerable undulator gap (*e.g.* >7 mm for out-of-vacuum devices), an optical cavity is commonly hosted in <2 GeV energy rings (see also Fig. 3). Lasing at wavelengths shorter than ∼150 nm becomes accessible in single-pass external-laser-seeding schemes, as described in the preceding sub-section.

4. Storage-ring-driven high-gain FEL

4.1. Motivations

A cutting-edge perspective is offered by a storage-ring-driven high-gain FEL (SR-HG-FEL), first proposed by Murphy & Pellegrini (1985). The advantage of a SR-HG-FEL, here intended to be lasing in the EUV and soft X-ray wavelength range, becomes evident as long as an existing storage-ring infrastructure is already in place or planned. It is clear, indeed, that by exploiting a stored beam at GeV-beam energy level for lasing would save from a few tens to many hundreds of million euros, otherwise required for the construction of a 1 to ∼5 GeV high-brightness normal-conducting electron linac, including buildings and all related accelerator components. The linac total cost would reach the billion euro level for superconducting RF technology, typically requested for high FEL pulse repetition rate. A SR-HG-FEL would take advantage of the multi-bunch filing pattern of the storage ring, thereby being able to provide from kHz to MHz-range photon-pulse repetition rate with no additional superconducting RF components. Expected performance and limitations of such a light source are discussed in the following.

4.2. SASE-FEL concept

Electron-beam energies higher than 2 GeV and flat or round beams with horizontal natural emittance in the range 0.1–1 nm rad are compatible with lasing at fundamental wavelengths in the EUV and soft X-ray range. The exponential growth of the FEL power along the undulator adds three additional prerequisites to the electron-beam quality: bunch peak current higher than ∼0.5 kA, slice relative energy spread lower than ∼0.1%, and room for an undulator as long as several tens of meters (an option for CHG with a short radiator is discussed later on). Such a long undulator can only be accommodated in a line separated from the ring, henceforth named by-pass, and selected bunches have to be extracted from the ring without interference with nearby bunches. If internal to the ring, the by-pass line may imply re-injection of the FEL-spent beam into the synchrotron.

In one of the very first conceptual designs of a storage-ring-driven by-pass FEL (Kim *et al.*, 1985), the ring was devoted to single-bunch operation at relatively high peak current, and therefore the FEL emission was not compatible with the standard multi-bunch synchrotron operation. In a recent proposal of ours (De Mitri & Cornacchia, 2015, and references therein), single-bunch peak currents comparable with those achieved in RF linacs can be obtained through magnetic-bunch length compression. In that proposal, beam gymnastics are carried out *inside* the storage ring, and therefore limited by the RF cavity impedance and the large momentum compaction implied by the compression scheme.

Here, we imagine that, *after extraction* from the main ring, a linac of length a few meters at ∼20 MV m^{-1} accelerating gradient and 100 MV peak-voltage level is followed by a relatively long arc compressor, see Fig. 4. The arc injects in turn the time-compressed beam into the undulator line. Preservation of beam transverse emittance in the presence of coherent synchrotron radiation in the arc dipole magnets is ensured by a suitable optics arrangement. Sextupole magnets are included in the arc in order to linearize the compression process and, meanwhile, cancel higher-order chromatic aberrations (see Mitri & Cornacchia, 2015, and references therein).

For bunch-length compression by a factor of ∼10, beam energy spread at 1% is expected at the undulator, which largely exceeds the typical FEL energy bandwidth of ∼0.1%.

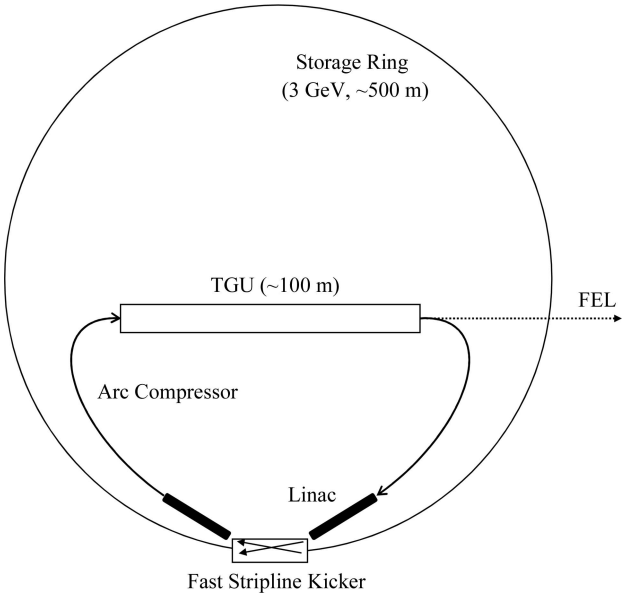

Figure 4
Schematic of a storage ring light source with undulator in a by-pass line. Electron bunches, stored in the ring in standard multi-bunch filling pattern, are kicked into the FEL loop by a fast stripline kicker plus septum system, hosted in a straight section of length a few meters. A linear energy correlation is imparted along the bunch (energy chirp) by an RF linac ('chirper') of length a few meters, which lies internally to the ring. The beam is then magnetically time-compressed in a 100 m-long, 100° arc compressor, and transported to the 100 m-long undulator line. The beam reaches the undulator entrance at full compression. Lasing occurs in a vertical TGU, which is preceded and followed by small vertical dog-legs (not shown) that manage some of the vertical energy dispersion function in the undulator for optimum FEL efficiency. The beam is extracted from the TGU and decompressed in time in the second arc. Another short RF linac acts as a 'dechirper', so that the beam-phase space rotation is completed at its exit, and the beam has recovered its initial peak current and energy distribution. The beam is finally injected back into the ring, and stored for providing light to ID beamlines, until next extraction.

The energy spread mismatch can be overcome by a transverse gradient undulator (TGU) traversed by an energy-dispersed beam (Smith *et al.*, 1979; Huang *et al.*, 2012). The field gradient (realistic magnetic designs suggest up to 100 m^{-1} field relative variation per unit distance from the undulator axis) and the energy-dispersion function (typically at ∼1 cm level) through the TGU shall match a condition for resonant emission from all the electrons. While the construction of TGU modules with relatively high field gradients and full polarization control is already on-going (Calvi *et al.*, 2017), the electron-beam transport through a line made of tens of such segments raises the challenge of beam-envelope control. The simplest scenario considered so far in the literature is that of a quadrupole-free beamline, at the expense of larger average electron-beam sizes and reduced FEL power (Cai *et al.*, 2013). In the following, this option will be considered for a numerical estimation of the TGU-FEL performance.

If the FEL-spent bunches were dumped after lasing, the synchrotron light source should be replenished at relatively short intervals, with frequent interruption of the standard operation. An alternative option, transparent to the standard multi-bunch operation of the ring, sees the FEL-spent bunches re-injected into the ring through an arc (de-)compressor-plus-linac beamline, identical and symmetric to the one devoted to lasing. Beam extraction and injection systems fast enough to approach the typical separation of RF buckets at the nanosecond time scale, together with kicker pulse durations up to ∼100 ns (for either single-bunch or bunch train extraction), are nowadays under development for the implementation of swap-out injection schemes in DLSRs (Pappas *et al.*, 2016), and are therefore within the reach of the proposed scheme.

4.3. SASE-FEL numerical results

Lasing in the high-gain regime implies a dilution of the electron-beam six-dimensional phase space, primarily through an increased energy spread, proportional to the FEL energy efficiency, and an enlarged transverse emittance, since photons are emitted by electrons traveling on energy-dispersive trajectories in the TGU. As the lasing bunches are re-injected into the ring, synchrotron radiation damping contributes to washing out the FEL perturbation. If lasing occurs at time intervals longer than a few damping times, the FEL is expected to behave as a single-pass light source, and the equilibrium beam distribution in the synchrotron is recovered between consecutive lasing. In this case, the performance of a self-amplified spontaneous emission (SASE) FEL (Kondratenko & Saldin, 1980; Bonifacio *et al.*, 1984) reaching power saturation in a TGU can be estimated analytically according to the model presented by Huang *et al.* (2008). The exponential growth of FEL power through the TGU is determined by a gain length defined as follows,

$$L_{g,\mathrm{TGU}} = \frac{\lambda_u}{4\pi\sqrt{3}\,\rho_{\mathrm{TGU}}}\left[1+\left(\frac{\sigma_{\delta,\mathrm{ef}}}{\rho_{\mathrm{TGU}}}\right)^2\right]. \qquad (4)$$

Here, $\sigma^2_{\delta,\mathrm{ef}} = (\sigma^2_{\delta,u})/\{1+[(\overline{\eta}\sigma_{\delta,u})/\overline{\sigma}_{y,\beta}]^2\}$, and $\overline{\eta}_y$ and $\overline{\sigma}_{y,\beta}$ are the average value of the vertical dispersion function and r.m.s. betatron beam size along the undulator, respectively, $\sigma_{\delta,u}$ is the beam r.m.s. relative energy spread at the undulator entrance, and $\rho_{\mathrm{TGU}} = \rho_{1D}/[1+(\bar{\eta}_y\sigma_{\delta,u}/\bar{\sigma}_{y,\beta})^2]^{1/6}$. The one-dimensional FEL parameter is defined, for example, by Bonifacio *et al.* (1984). Table 2 summarizes the expected performance of a high-gain TGU-FEL in a ∼500 m-long circumference, 3 GeV beam-energy storage ring. These results are based on particle tracking with the *elegant* code (Borland, 2000) in the main ring, and on analytical estimation of the FEL performance in a quadrupole-free TGU line (Baxevanis *et al.*, 2014) starting from tracked electron-beam parameters. The ring lattice is based on a four-bend achromatic cell and it approaches the diffraction limit in the horizontal (vertical) plane at a wavelength of 6 nm (0.03 nm). A 0.1 kHz repetition-rate stripline kicker is considered with 50 ns flat-top pulse duration (25 bunches per kicker pulse). The FEL pulse repetition rate is 2.5 kHz, assuming 100 Hz damping rate in the storage ring and ∼100 stored bunches. At the fundamental

Table 2
Parameters of the 3 GeV storage-ring high-gain SASE-FEL.

Synchrotron light source			Units
Mean beam energy	3.0		GeV
Circumference length	528		m
Achromatic cell type	Four-bend		
Revolution period	1.76		μs
Harmonic number	880		
RF bucket spacing	2		ns
Longitudinal damping time	9		ms
Bunch charge	1.0		nC
Bunch duration, r.m.s.	9		ps
Peak current	44		A
Relative energy spread, r.m.s.	0.08		%
Transverse geometric emittance, r.m.s. (x, y)	500, 2.5		pm rad
Arc compressor			
Arc cell type	Triple-bend achromat		
Number of cells	4		
Total deflection angle	108		°
Total length	104		m
Final relative energy spread, r.m.s.	1.4		%
Bunch duration at FEL, r.m.s.	0.55		ps
Peak current at FEL	715		A
Final geometric emittance (x, y)	570, 5		pm rad
TGU-FEL			
Undulator parameter	4		
Undulator period	90		mm
Total undulator length	100		m
TGU gradient	100		m^{-1}
Average vertical dispersion in TGU	10		mm
Average (β_x, β_y) along TGU	15, 70		m
Average beam size along TGU, r.m.s. (x, y)	90, 180		μm
FEL fundamental wavelength	13.0		nm
FEL pulse length, r.m.s.	0.5		ps
TGU-FEL parameter	0.15		%
FEL pulse repetition rate	2.5 (burst)	20×10^3 (burst)	kHz
TGU-FEL gain length	5	8	m
TGU-FEL saturation length	100	155	m
FEL peak power, per pulse	1×10^3	1.5	MW
FEL energy, per pulse	570	0.8	μJ
Number of photons, per pulse	2×10^{14}	3×10^{11}	
Number of FEL pulses per train	25	50	
FEL average power, total	2.5	30	W

lasing wavelength of 13 nm, the saturation length is ∼100 m, and the saturation power is ∼1 GW.

In a second scenario, also listed in Table 2, a 400 kHz repetition-rate stripline kicker is considered; 100 ns flat-top pulse duration hosts now 50 bunches per kicker pulse. Rise and fall times of the kicker are estimated at the 5 ns level, and we assume a hybrid filling pattern in the ring with at least three long bunch trains separated by 10 ns or so. The kicker is assumed to work in burst mode and the corresponding FEL pulse repetition rate turns out to be 2 MHz. Unfortunately, in this scenario the vertical beam emittance growth due to chromatic effects in the TGU cannot be washed out efficiently, as long as we assume that the FEL repetition rate is higher than the vertical radiation damping time. It thereby leads to a rapid degradation in the FEL energy efficiency. The upper limit to the emittance growth at each pass in the TGU is estimated as

$$\varepsilon_{y,i}^2 \simeq \varepsilon_{y,i-1}^2 \left[1 + \frac{(\overline{\eta}_y \sigma_{\delta,\mathrm{FEL}})^2}{\varepsilon_{y,i-1}\, \overline{\beta}_y} \right], \quad (5)$$

where the emittance at the end of the TGU is proportional to the emittance at its entrance, to the average vertical dispersion function through the TGU, to the FEL-induced energy spread, and inversely proportional to the average vertical betatron function. With the values in Table 2, the FEL intensity is expected to drop in a few loops, well before one damping time. With respect to the single-pass behavior mentioned above, the peak power is reduced by three orders of magnitude. The average FEL power is, nevertheless, still considerable. The FEL output single-pulse peak power is calculated for each pass through the TGU on the basis of the analytical model introduced by Huang *et al.* (2008). After each pass, the beam energy spread growth due to lasing is calculated, as well as the emittance growth. These data are used to modify the electron-beam distribution that is tracked with *elegant* through the ring and the arcs. The beam parameters resulting from tracking and evaluated at the entrance of the undulator are newly used for the analytical evaluation of the FEL performance, and so on. Fig. 5 shows that after a number of loops corresponding to about half the damping time the FEL power is already so low that the nominal equilibrium electron-beam parameters are basically unaffected by lasing. In other words, lasing shifts out of the power-saturation regime in less than the damping time. At equilibrium, the FEL pulse peak power is at the 1 MW level at a repetition rate as high as 1 MHz. It is worth stressing that the high-repetition-rate scenario may imply average beam currents above 1 mA in the linac sections. A choice is here imposed between high average beam current in the linac, thus high average FEL power, at the expense of superconducting RF technology, and reduced average FEL power with normal conducting linac sections.

4.4. Seeded FEL and CHG

The proposed SR-HG–FEL scheme opens the door to external seeding schemes for improved longitudinal coherence and CHG. Since the electron-beam parameters at the undulator are in the same ballpark of existing seeded FEL facilities, both high-gain harmonic generation (Yu, 1991; Allaria *et al.*, 2012) and echo-enhanced harmonic generation (Stupakov,

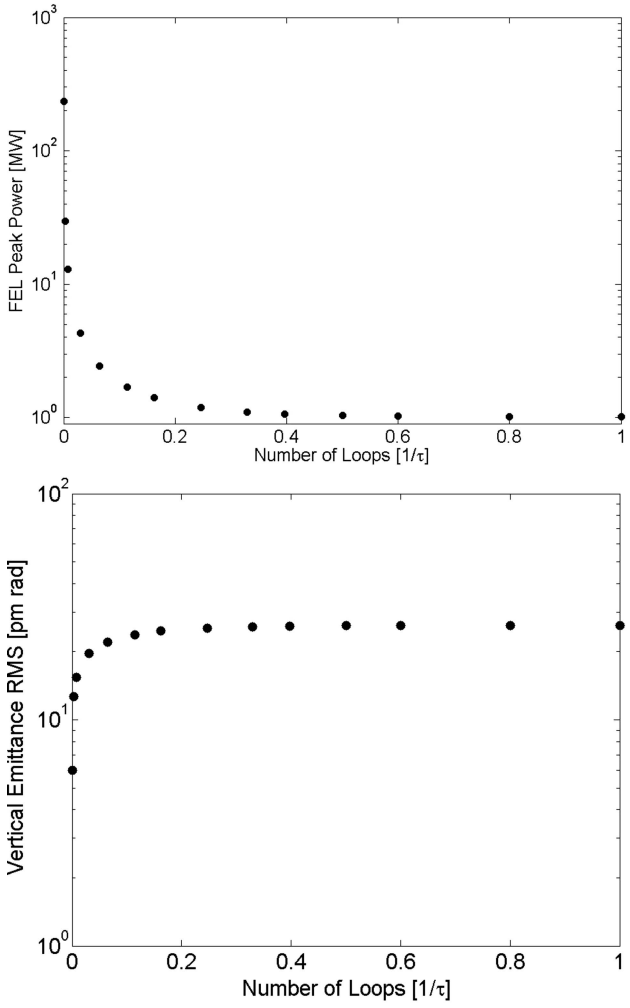

Figure 5
Top: TGU-based SASE-FEL single-pulse peak power as a function of the number of storage-ring FEL loops in units of longitudinal damping time, when each bunch is lasing every 1.5 revolution periods in the storage ring (the by-pass line-pulse-arcs beamline is assumed to cover a length equal to half of the ring circumference). FEL gain is rapidly suppressed by the growth of beam vertical emittance in the TGU, whose evolution is shown at the bottom. The low FEL peak power reached at equilibrium minimally disturbs the beam longitudinal emittance in the storage ring.

2009; Zhao *et al.*, 2012) are conceivable. Such seeding schemes, generally considered in linac-driven FELs, can be translated to the case of large-energy-spread beams in the configuration of phase-merging harmonic generation (Feng *et al.*, 2014). This is basically an optical manipulation of the electron beam passing through a TGU with non-zero dispersion, which allows for high harmonic jumps. The aforementioned seeding options are to date the only viable ways to approach full coherent pulses at soft X-ray wavelengths, most likely down to 1 nm or so. For all the seeding schemes, the FEL pulse repetition rate would be limited by the UV-laser repetition rate. At 1 kHz seeding frequency, we expect a FEL performance intermediate to those reported in Table 2, but now with full transverse and longitudinal coherence.

A simpler scenario foresees a few meters-long TGU segment for CHG. The reduced FEL flux would be partially compensated by a tighter electron beam focusing through the short TGU line. Since the bunch peak current is high, $\sim 10^8$ photons per pulse at ~ 10 nm are expected with ~ 100 kHz photon-pulse repetition rate, and a pulse duration of the order of 0.1 ps FWHM.

5. Comparison of performance

Table 3 summarizes our discussion on the compatibility of the aforementioned techniques for production of picosecond and sub-picosecond X-ray pulses in synchrotron light sources with standard multi-bunch user mode (SUM) and with diffraction limit electron optics (DLO). The photon-pulse peak intensity (number of photons per pulse) for all different short-pulse options was estimated as follows: for those schemes in which the electron beam radiates in standard IDs, the intensity is scaled linearly proportional to the bunch charge and the photon-pulse duration; for schemes relying on dedicated IDs and limited to some minimum wavelength, the intensity is relative to the SUM intensity intended as emission at the minimum wavelength in a hybrid 2 m-long undulator from a 40-ps-FWHM-long electron bunch and 1 nC bunch charge.

Our present understanding highlights a major incompatibility of the low-alpha operating mode with DLO. Although, in principle, some compatibility could be envisioned for the other techniques from the pure beam dynamics perspective, practical conflicts for available space and optics tuning emerge when new hardware has to be installed internal to the ring, such as in the case of beam deflection. Voltage beating may have more chances of compatibility with DLO because it primarily deals with a manipulation of the longitudinal beam dynamics, whereas DLO imposes stronger constraints on the transverse one. On the one hand, a reduction by at least one order of magnitude in radiation intensity, compared with that emitted in SUM, is foreseen in this case; a lower bunch charge is dictated by the microwave instability threshold for short bunches. On the other hand, a reduced charge in short bunches would alleviate the emittance growth induced by intra-beam scattering at low-emittance values. The most recent proposal of CHG with optics manipulation of the electron beam for enhanced bunching factor is compatible with SUM as long as a relatively low peak current is accepted. While this scheme promises at least one order of magnitude higher flux than in femto-slicing and other standard CHG configurations, the special optics design required for bunching enhancement looks to be in conflict with DLO. The storage-ring-driven high-gain FEL is compatible with both SUM and DLO because it decouples by design the electron-beam gymnastic devoted to lasing from the electron-beam gymnastics in the storage ring. This is, however, at the expense of the installation of short linacs and arc compressors internal to the ring. For completeness, indicative parameters of state-of-the-art high-harmonic-generation (HHG) light sources in gas are also given (Hädrich *et al.*, 2016). Table 4 highlights the potential of some of the mentioned schemes with regards to output radiation control.

Table 3
Summary of schemes for the generation of stable short X-ray pulses in synchrotron light sources, and estimated performance.

In the columns, from left to right: minimum FWHM photon-pulse duration, photon-pulse peak intensity relative to SUM, maximum pulse repetition rate, layout-invasive (important modifications to the synchrotron lattice or occupancy of more than one straight section), compatibility with SUM (see §5), compatibility with DLO design strategies, number of photon beamlines served simultaneously and approximate cost assuming an existing SRLS infrastructure. Indicative parameters of state-of-the-art HHG sources are also given (Hädrich *et al.*, 2016). Numbers are intended as indicative of the order of magnitude.

	Δt_{min} (ps)	I/I_{SUM}	RR_{max} (MHz)	Layout-invasive	Compatible with SUM	Compatible with DLO	Beamlines	Cost (M euros)
Low-alpha	2	10^{-2}	500	No	No	No	All	<1
Harmonic cavity	1–10	10^{-2}–1	500	No	Yes†	Yes‡	All	<1
RF voltage beating	1	10^{-2}–10^{-1}	500	Yes	Yes	Maybe‡	All	20
RF deflector	2	10^{-6}–1	500	Yes	Yes	Unlikely	1 to all	10
Femto-slicing	0.1	10^{-7}–10^{-4}	0.1	No	Yes	Maybe‡	1	2
Optical cavity§	20	10^{-2}	1	No	No	No	1	2
CHG (OK/others)¶	0.1	$<10^{2}$	0.1	No/Yes	No	Unlikely‡	1	1
TGU-FEL (SASE)††	3	10^{-3}–10^{6}	1–100	No	Yes	Yes	1	5–30
TGU-FEL (seed)††	0.1	10^{-4}–10^{5}	0.1	No	Yes	Yes	1	5–30
HHG††	1	10^{-2}–10^{2}	10	–	–	–	1	5

† If low-alpha optics is not adopted. In this case the minimum FWHM pulse duration is expected at the 10 ps level. ‡ For storage rings at beam energy lower than ∼3 GeV. § Limited to fundamental wavelengths of emission >150 nm. ¶ Limited to fundamental wavelengths of emission >10 nm. †† Limited to fundamental wavelengths of emission >1 nm.

Table 4
Comparison of the estimated performance of schemes for the generation of short photon pulses in storage rings (see also Table 3).

Indicative parameters of state-of-the-art HHG sources are also given (Hädrich *et al.*, 2016).

	λ_{min} (nm)	λ-tunability	Polarization	Spectral bandwidth (FWHM) (%)	Coherence, transverse/longititudinal	e-Beam energy (GeV)
Femto-slicing	∼0.1	Wide	Variable	>0.1†	Incoherent†	<3
CHG	∼10	Wide	Variable	>0.1	Poor/Poor	<3
TGU-FEL (SASE)	∼4	Small	Variable	∼0.1	High/Poor	<5
TGU-FEL (seed)	∼4	Small	Variable	0.01–0.1	High/High	<5
HHG	∼4	Wide	Linear	∼0.1	High/High	–

† Photon emission occurs at standard IDs by incoherent processes. The bandwidth is typically larger than in all other schemes on the list.

6. Conclusions

The interest of the scientific community for picosecond and sub-picosecond EUV and X-ray pulses in synchrotron light sources is recalled, looking, for example, to the development of synchrotron light sources in the last 40 years, and compared with the performance of state-of-the-art linac-driven FELs. The compatibility of schemes for the production of short pulses in synchrotrons with standard multi-bunch operation and diffraction-limited optics design is discussed. Such a discussion is established on the basis of scaling laws for the beam horizontal emittance *versus* beam energy, taking into consideration multi-bend lattice complexity and the trend of storage ring circumference with energy. By keeping Fig. 2, Table 3 and Table 4 in mind, we can preliminary conclude that synchrotron light sources at beam energies lower than ∼3 GeV might attempt a combined diffraction-limited emittance short-pulse operation. An absolute value of the natural horizontal emittance in the range 0.1–0.5 nm would be sufficient for approaching the diffraction limit in the EUV and soft X-ray wavelength range. At the same time, short X-ray pulses might be obtained *via* the RF voltage beating technique (1–3 ps FWHM duration, in principle compatible with lower-emittance values), RF vertical deflection or CHG (0.1–1 ps FWHM duration, with some higher emittance because of large betatron amplitude optics in limited machine regions). The high-gain TGU-FEL scheme was proposed with the primary aim of full compatibility with SUM and DLO. This is actually the only scheme, among all those discussed, which takes advantage of reduced emittance values of the stored beam. The main limitation in extending this scheme to hard X-rays comes from the emittance degradation during lasing, which is expected at very high repetition rates. A variety of intermediate scenarios is offered by this scheme as a function of wavelength of emission, seeding scheme, photon flux and average FEL power. A detailed report demonstrating the technical feasibility of the proposed solution will be given in a separate work.

Acknowledgements

C. Masciovecchio, D. Fausti, B. Diviacco and D. Garzella are acknowledged for stimulating discussions and helpful insights. M. Cornacchia is acknowledged for insights on the beam dynamics at equilibrium in the presence of lasing in a by-pass.

References

Allaria, E., Appio, R., Badano, L., Barletta, W. A., Bassanese, S., Biedron, S. G., Borga, A., Busetto, E., Castronovo, D., Cinquegrana, P., Cleva, S., Cocco, D., Cornacchia, M., Craievich, P., Cudin,

I., D'Auria, G., Dal Forno, M., Danailov, M. B., De Monte, R., De Ninno, G., Delgiusto, P., Demidovich, A., Di Mitri, S., Diviacco, B., Fabris, A., Fabris, R., Fawley, W., Ferianis, M., Ferrari, E., Ferry, S., Froehlich, L., Furlan, P., Gaio, G., Gelmetti, F., Giannessi, L., Giannini, M., Gobessi, R., Ivanov, R., Karantzoulis, E., Lonza, M., Lutman, A., Mahieu, B., Milloch, M., Milton, S. V., Musardo, M., Nikolov, I., Noe, S., Parmigiani, F., Penco, G., Petronio, M., Pivetta, L., Predonzani, M., Rossi, F., Rumiz, L., Salom, A., Scafuri, C., Serpico, C., Sigalotti, P., Spampinati, S., Spezzani, C., Svandrlik, M., Svetina, C., Tazzari, S., Trovo, M., Umer, R., Vascotto, A., Veronese, M., Visintini, R., Zaccaria, M., Zangrando, D. & Zangrando, M. (2012). *Nat. Photon.* **6**, 699–704.

Bartolini, R., Borland, M. & Harkay, K. (2006). *Proceedings of the Tenth European Particle Accelerator Conference (EPAC'2006)*, 26–30 June 2006, Edinburgh, Scotland, p. 160. MOPCH054.

Baxevanis, P., Ding, Y., Huang, Z., Ruth, R. (2014). *Phys. Rev. ST Accel. Beams*, **17**, 020701.

Bazarov, I. V. (2012). *Phys. Rev. ST Accel. Beams*, **15**, 050703.

Bonifacio, R., Pellegrini, C. & Narducci, L. M. (1984). *Opt. Commun.* **50**, 373–378.

Borland, M. (2000). *Elegant: a Flexible SDDS-Compliant Code for Accelerator Simulation.* Technical Report LS-287. Advanced Photon Source, Argonne, IL, USA.

Borland, M. (2014). *Synchrotron Radiat. News*, **27**(6), 2–3.

Cai, Y., Ding, Y., Hettel, R., Huang, Z., Wang, L., Xiao, L. (2013). *Synchrotron Radiat. News.* **26**(3), 39–41.

Calvi, M., Camenzuli, C., Prat, E. & Schmidt, T. (2017). *J. Synchrotron Rad.* **24**, 600–608.

Chin, Y. H. (1990). *Presented at the International Workshop on Accelerators for Asymmetric B-Factories*, 4–6 October 1990, Tsukuba, Japan. LBL-29622.

Couprie, M. E. (1997). *Nucl. Instrum. Methods Phys. Res. A*, **393**, 13–17.

Dattoli, G., Di Pace, A., Mezi, L. & Sabia, E. (1998). *J. Appl. Phys.* **83**, 5034–5039.

De Mitri, S. & Cornacchia, M. (2015). *New J. Phys.* **17**, 113006.

De Ninno, G., Allaria, E., Coreno, M., Curbis, F., Danailov, M. B., Karantzoulis, E., Locatelli, A., Menteş, T. O., Nino, M. A., Spezzani, C. & Trovò, M. (2008). *Phys. Rev. Lett.* **101**, 053902.

Einfeld, D., Schaper, J. & Plesko, M. (1995). *Proceedings of the 1995 Particle Accelerator Conference*, 1–5 May 1995, Dallas, TX, USA, pp. 177–179. TPG08.

Evain, C., Loulergue, A., Nadji, A., Filhol, J. M., Couprie, M. E. & Zholents, A. A. (2012). *New J. Phys.* **14**, 023003.

Feikes, J., Holldack, K., Kuske, P. & Wüstefeld, G. (2004). *Proceedings of the Ninth European Particle Accelerator Conference (EPAC'04)*, 5–9 July 2004, Lucerne, Switzerland, p. 1954. WEPLT051.

Feng, C., Deng, H., Wang, D. & Zhao, Z. (2014). *New J. Phys.* **16**, 043021.

Feng, C. & Zhao, Z. (2017). *Sci. Rep.* **7**, 4724.

Fritz, D. M. & Yabashi, M. (2017). *Synchrotron Radiat. News*, **30**(6), 2.

Hädrich, S., Rothhardt, J., Krebs, M., Demmler, S., Klenke, A., Tünnermann, A. & Limpert, J. J. (2016). *J. Phys. B At. Mol. Opt. Phys.* **49**, 172002.

Hettel, R. (2014). *Proceedings of the 5th International Particle Accelerator Conference (IPAC'2014)*, 15–20 June 2014, Dresden, Germany, p. 7. MOXBA01.

Höppner, H., Hage, A., Tanikawa, T., Schulz, M., Riedel, R., Teubner, U., Prandolini, M. J., Faatz, B. & Tavella, F. (2015). *New J. Phys.* **17**, 053020.

Huang, Z., Bane, K., Cai, Y., Chao, A., Hettel, R. & Pellegrini, C. (2008). *Nucl. Instrum. Methods Phys. Res. A*, **593**, 120–124.

Huang, Z., Ding, Y. & Schroeder, C. B. (2012). *Phys. Rev. Lett.* **109**, 204801.

Jankowiak, A., Anders, W., Atkinson, T., Ehmler, H., Föhlisch, A., Goslawski, P., Holldack, K., Knobloch, J., Kuske, P., Malyutin, D., Matveenko, A. N., Müller, R., Neumann, A., Ott, K., Ries, M., Ruprecht, M., Schälicke, A., Vélez, A. V. & Wüstefeld, G. (2016) *Proceedings of the 7th International Particle Accelerator Conference (IPAC'2016)*, 8–13 May 2016, Busan, Korea, p. 2833. WEPOW009.

Kim, K.-J., Bisognano, J. J., Garren, A. A., Halbach, K. & Peterson, J. M. (1985). *Nucl. Instrum. Methods Phys. Res. A*, **239**, 54–61.

Kim, K.-J., Huang, Z. & Lindberg, R. (2017). *Synchotron Radiation and Free-Electron Lasers*, pp. 12–32, Cambridge University Press.

Kondratenko, A. M. & Saldin, E. L. (1980). *Partic. Accel.* **10**, 207–216.

Leemann, S. (2014). *Phys. Rev. ST Accel. Beams*, **17** 050705.

Liu, L. & Westfahl, H. Jr (2017). *Proceedings of the 8th International Particle Accelerator Conference (IPAC'2017)*, 14–19 May 2017, Copenhagen, Denmark, p. 1203. TUXA1.

Martin, I. P. S. (2011). PhD Thesis, Wolfson College, University of Oxford, UK (https://ora.ox.ac.uk/objects/uuid:9ac0bcc2-bedb-46d0-b95c-22f4741f45a0).

Martin, I., Rehm, G., Thomas, C. & Bartolini, R. (2011). *Phys. Rev. ST Accel. Beams*, **14**, 040705

Murphy, J. B. & Pellegrini, C. (1985). *Nucl. Instrum. Methods Phys. Res. A*, **237**, 159–167.

Pappas, C., De Santis, S., Jung, J.-Y., Luo, T. H., Steier, C., Swenson, C. A. & Waldron, W. L. (2016). *Proceedings of the 7th International Particle Accelerator Conference (IPAC'2016)*, 8–13 May 2016, Busan, Korea, p. 3637. THPMW038

Prince, K., Allaria, E., Callegari, C., Cucini, R., De Ninno, G., Di Mitri, S., Diviacco, B., Ferrari, E., Finetti, P., Gauthier, D., Giannessi, L., Mahne, N., Penco, G., Plekan, O., Raimondi, L., Rebernik, P., Roussel, E., Svetina, C., Trovò, M., Zangrando, M., Negro, M., Carpeggiani, P., Reduzzi, M., Sansone, G., Grum-Grzhimailo, A. N., Gryzlova, E. V., Strakhova, S. I., Bartschat, K., Douguet, N., Venzke, J., Iablonskyi, D., Kumagai, Y., Takanashi, T., Ueda, K., Fischer, A., Coreno, M., Stienkemeier, F., Ovcharenko, Y., Mazza, T. & Meyer, M. (2016). *Nat. Photon.* **10**, 176–179.

Reis, D. R. (2016). *Synchrotron. Radiat. News*, **29**(5), 2.

Robin, D., Forest, E., Pellegrini, C. & Amiry, A. (1993). *Phys. Rev. E*, **48**, 2149–2156.

Schoenlein, R. W., Chattopadhyay, S., Chong, H. H., Glover, T. E., Heimann, P. A., Shank, C. V., Zholents, A. A. & Zolotorev, M. S. (2000). *Science*, **287**, 2237–2240.

Smith, T., Madey, J. M. J., Elias, L. R. & Deacon, D. A. G. (1979). *J. Appl. Phys.* **50**, 4580–4583.

Stupakov, G. (2009). *Phys. Rev. Lett.* **102**, 074801.

Trovò, M., Clarke, J. A., Couprie, M. E., Dattoli, G., Garzella, D., Gatto, A., Giannessi, L., Günster, S., Kaiser, N., Marsi, M., Poole, M. W., Ristau, D. & Walker, R. P. (2002). *Nucl. Instrum. Methods Phys. Res. A*, **483**, 157–161.

Williams, G. P. & Herman, W. (2015). *Synchotron Radiat. News*, **28**(4), 2–3.

Wüstefeld, G., Jankowiak, A., Knobloch, J. & Ries, M. (2011). *Proceedings of the Second International Particle Accelerator Conference (IPAC'2011)*, 4–9 September 2011, San Sebastián, Spain, p. 2936. THPC014.

Yu, L. H. (1991). *Phys. Rev. A*, **44**, 5178–5193.

Zhao, Z. T., Wang, D., Chen, J. H., Chen, Z. H., Deng, H. X., Ding, J. G., Feng, C., Gu, Q., Huang, M. M., Lan, T. H., Leng, Y. B., Li, D. G., Lin, G. Q., Liu, B., Prat, E., Wang, X. T., Wang, Z. S., Ye, K. R., Yu, L. Y., Zhang, H. O., Zhang, J. Q., Zhang, M., Zhang, M., Zhang, T., Zhong, S. P. & Zhou, Q. G. (2012). *Nat. Photon.* **6**, 360–363.

Zholents, A. (2015). *Nucl. Instrum. Methods Phys. Res. A*, **798**, 111–116.

Zholents, A., Heimann, P., Zolotorev, M. & Byrd, J. (1999). *Nucl. Instrum. Methods Phys. Res. A*, **425**, 385–389.

Zholents, A. A. & Zolotorev, M. S. (1996). *Phys. Rev. Lett.* **76**, 912–915.